Journal of Physics: Condensed Matter

PAPER

n-type Rashba spin splitting in a bilayer inorganic halide perovskite with external electric field

To cite this article: Xuejiao Chen *et al* 2018 *J. Phys.: Condens. Matter* **30** 265501

View the article online for updates and enhancements.

Related content

- Switchable Rashba effect by dipole moment switching in an Ag2Te monolayer
Mohammad Noor-A-Alam, Minseong Lee, Hyun-Jae Lee et al.
- Polarized emission in II-VI and perovskite colloidal quantum dots
Maya Isarov, Liang Z Tan, Jenya Tilchin et al.
- Gate induced monolayer behavior in twisted bilayer black phosphorus
Cem Sevik, John R Wallbank, Ouz Gülseren et al.

IOP ebooks™

Bringing you innovative digital publishing with leading voices to create your essential collection of books in STEM research.

Start exploring the collection - download the first chapter of every title for free.

This content was downloaded from IP address 159.226.100.205 on 20/05/2019 at 07:53

IOP Publishing Journal of Physics: Condensed Matter
J. Phys.: Condens. Matter **30** (2018) 265501 (5pp) https://doi.org/10.1088/1361-648X/aac523

n-type Rashba spin splitting in a bilayer inorganic halide perovskite with external electric field

Xuejiao Chen[1,2], **Lei Liu**[1] **and Dezhen Shen**[1]

[1] State Key Laboratory of Luminescence and Applications, Changchun Institute of Optics, Fine Mechanics and Physics, Chinese Academy of Sciences, No.3888 Dongnanhu Road, Changchun 130033, People's Republic of China
[2] University of Chinese Academy of Sciences, Beijing 100049, People's Republic of China

E-mail: liulei@ciomp.ac.cn and shendz@ciomp.ac.cn

Received 10 April 2018, revised 4 May 2018
Accepted for publication 14 May 2018
Published 5 June 2018

Abstract

Here, we investigated the Rashba effect of the $CsPbBr_3$ bilayers under the external electric field (EEF) with first-principles calculations. For the $PbBr_2$ terminated bilayer, we found that only electrons experience the Rashba splitting under EEF, while holes do not. Such an n-type Rashba effect can be ascribed to the surface relaxation effect that reverses the positions of the top valence bands. The n-type Rashba parameter can be tuned monotonically to the maximum of 0.88 eV Å at EEF of 1.35 V nm^{-1} at which the sequence of top valence bands recover to the bulk style. During this process the p-type spins will not survive in this 2D $CsPbBr_3$, that indeed reveals a new way for making advanced functional spintronic devices.

Keywords: Rashba spin–orbit coupling, halide perovskite, density functional theory, external electric field

S Supplementary material for this article is available online

(Some figures may appear in colour only in the online journal)

1. Introduction

Recently, the halide perovskites have aroused great research interests in different areas, such as photovoltaics, optoelectronics, or even catalysis and electrocatalysis [1–3], and so on. That can be ascribed to their intrinsic merits, including proper bandgap, strong optical absorption, balanced carrier mobility, long carrier diffusion length, low exciton binding energy, and most of all defect tolerance [4–9]. While defect tolerance means these perovskites would be electronically inert from alien electronic states, that will certainly give them natural advantages in many device applications, where defects or interfaces are inevitable. Although being nonmagnetic, the halide perovskites can be fabricated into spintronic devices as well, in case enough spins can be produced and well controlled.

For those nonmagnetic semiconductors as perovskites, the spin degeneracy of their electronic bands can be removed by the with inverse-symmetry breaking operations and spin–orbit coupling (SOC), such as the Dresselhaus effect [10] typically in their bulk phases, or by the Rashba effect normally around their surfaces or heterostructure interfaces [11–21]. Approximately, this Rashba effect can be represented by the Hamiltonian [11, 18]: $H_R = \lambda\vec{\sigma}\cdot(\vec{E}_z \times \vec{k})$, where $\vec{\sigma}$ is the vector of the Pauli matrices, $\vec{E}_z$ is the electric field along the z axis normal to the slab surfaces, $\vec{k}$ is the electron momentum, and λ is the coupling constant. With this SOC term, the parabolic spin-degenerate band can split into two bands as $E^{\pm}(\vec{k}) = (\hbar^2\vec{k}^2/2m^*) \pm \alpha_R|\vec{k}|$, where m^* is the effective mass of electron or hole and α_R is the Rashba parameter. Therefore, around the band extremum points, such as conduction band minimum (CBM) or valance band maximum (VBM), the Rashba parameter can be calculated as:$\alpha_R = \frac{2\Delta E}{\Delta k}$, where Δk is the momentum offset and ΔE is the band extremum offset, as shown in figure 1.

 © 2018 IOP Publishing Ltd Printed in the UK

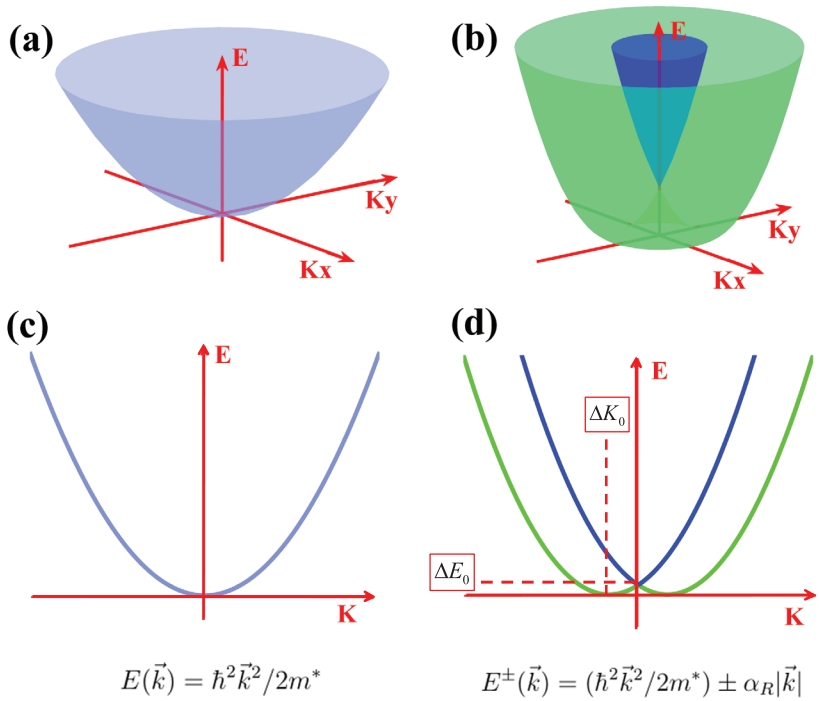

Figure 1. Schematic energy dispersion for (a), (c) double degenerate parabolic band and (b), (d) Rashba splitting band, respectively. The band structure of (a), (c) can be described as the equation : $E^{\pm}(\vec{k}) = \hbar^2\vec{k}^2/2m^*$. For (b), (d), this is : $E^{\pm}(\vec{k}) = (\hbar^2\vec{k}^2/2m^*) \pm \alpha_R|\vec{k}|$, where the Rashba parameter α_R is equal to $\frac{2\Delta E}{\Delta k}$. At the (b), (d), the blue band and green band have the opposite spin direction, which breaks the original spin-degenerate state.

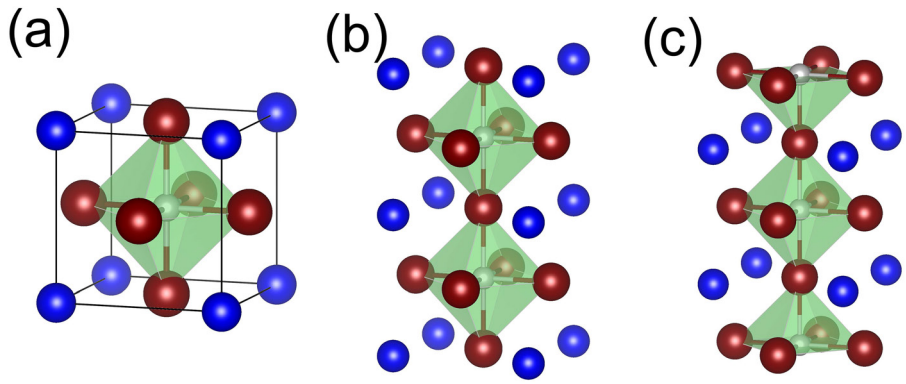

Figure 2. Crystal structures of $CsPbBr_3$ (a), CsBr-terminated (b) and $PbBr_2$-terminated (c) bilayers. (The blue balls represent Cs atoms, the gray balls represent Pb atoms while the brown balls represent Br atoms).

So far, the Rashba effect has been studied in many materials, including InAs quantum wells (QWs) [13, 14], $Al_xGa_{1-x}As$ QWs [15], bulk BiTeI [18] and GeTe [19], together with oxide perovskites [20, 22]. However, for halide perovskites, most of the works on Rashba splitting were on their organic–inorganic hybrid members [23–31]. While these halides suffer the stability problem [32], obviously it would be more meaningful to study the Rashba splitting on their more robust members, i.e. the all-inorganic halide perovskites.

Experimentally, the Rashba effect of all-inorganic halide perovskites has been observed by Maya *et al* on $CsPbBr_3$ nanocrystals based on the magneto-optical measurements at cryogenic temperatures [33]. This Rashba effect at the $CsPbBr_3$ nanocrystals may tune the electronic energy level to realize a bright triplet excitions [34]. But, for the real spintronic applications, its layer structures under electrical field would be of more interest to investigate. Indeed, by different groups [35, 36], the 2D layer structures of the $CsPbBr_3$ has been successfully synthesized from monolayer to several layers. However, for these layered halide perovskites, their Rashba performance under EEF has not been identified so far.

Here, with the relativistic first-principles density-functional theory (DFT) calculations, we studied the EEF-induced Rashba effect of the $CsPbBr_3$ bilayers terminated either with $PbBr_2$ or CsBr surfaces, as illustrated in figure 2. Two types of bilayers were found exhibiting distinct spin-splitting behaviors under EEF, i.e. the $PbBr_2$ one is a good Rashba material while the other is not.

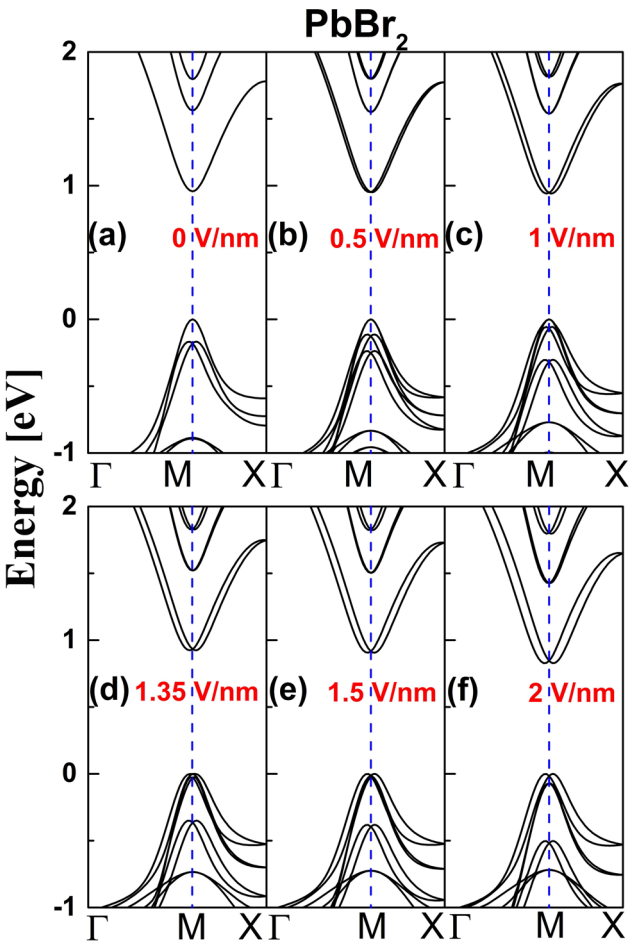

Figure 3. The calculated electronic band structures of the $PbBr_2$-terminated bilayer under different EEF.

2. Computational details

The DFT calculations on $CsPbBr_3$ bilayers were performed with the projector-augmented wave [37, 38] pseudopotentials and the Perdew–Burke–Ernzerhof [39] functional as implemented in the Vienna *Ab initio* Simulation Package [40, 41]. The experimental lattice parameters of the cubic phase $CsPbBr_3$ ($a = 5.874$ Å) [42], as shown in figure 2(a), were used to construct both $PbBr_2$ and CsBr terminated slabs, where the vacuum region was set as 15 Å. By setting the EEF normal to their surfaces, the atomic positions of both slabs were relaxed until their residual forces were less than 0.01 eV $Å^{-1}$. Here the electron wave function was expanded using plan waves with a kinetic-energy cutoff of 300 eV. K points were generated using the Monkhorst–Pack scheme with a mesh size of $6 \times 6 \times 1$. The calculated properties are corrected with SOC which is included by the second-variation method [43].

3. Results and discussion

3.1. Crystal structures

$CsPbBr_3$ in bulk, as shown in figure 2(a), has the symmetry of PM-3M. If cleaved along plane (0 0 1), its bilayer structures with thickness of $2a$ can be terminated with either CsBr or $PbBr_2$ atom layers, as shown in figures 2(b) and (c) respectively. While the CsBr-terminated bilayers are stacked with two identical intact $PbBr_6$ octahedron layers, the $PbBr_2$ ones are linked by the units of one center $PbBr_6$ octahedron and two half octahedra symmetrically in chain. Both $PbBr_2$ and CsBr bilayers still have the inversion symmetry, and they are nonpolar and charge neutral. As the EEF is applied perpendicular to their surfaces, the inversion symmetry can be switched off accordingly and that causes the Rashba effect. Moreover, the calculated total energies with/without EEF for two kinds of terminated surfaces clearly presents that the $PbBr_2$ terminated surface is more stable than CsBr case. Therefore, we mainly discuss the $PbBr_2$ terminated case.

3.2. Band structures and partial charge densities with EEF

Figure 3 presents the electronic bands around VBM and CBM with different EEFs for the $PbBr_2$ terminated bilayer. Obviously, its valence and the conduction bands behave differently upon EEF. Without EEF, both valance and conduction bands show the parabolic profiles around CBM and VBM repectively at M-point, as shown in figure 3(a). Once EEF turned on, these double-degenerate bands will split more or less as shown in figures 3(b)–(f). The lowest conduction band splits into two similar parabolic ones, with their new CBMs move away gradually from M-point to points Γ and X separately. In comparison, after splitting the top valence ones still share the VBM at M-point, where their profiles show different curvatures as shown in figures 3(b) and (c). That results in the holes possessing different effective masses. Moreover, with EEF, two bands just below VBM split vertically with one branch moving up and the other going down. As EEF is larger than 1.35 V nm^{-1}, the upper branch gets higher than the original top valence band. As this branch consists of two parabolic bands crossing each other at point M, that makes new VBM staying away from M-point.

To characterize the nature of these bands, we plotted their charge density distribution of CBM and VBM at three selected EEF values of 0, 1 and 2 V nm^{-1}, as shown in figure 4. Obviously, the CBM band comes from the extended p-orbitals of all Pb atoms. As shown in figure 4(a), the CBM states show the reflection symmetry about the central atomic layer. With EEF, the CBM charges becomes asymmetric, and their shapes on each Pb atom change from dumbbell-shape to spherical-like. In comparison, the initial VBM states, bonded with s-orbits of Pb and p-orbits of Br, distribute only on the central atomic layer of $PbCs_4$. As shielded by the surface electrons, such highly symmetric single-layer VBM states are not sensitive to EEF as shown in figure 4(b). Therefore, the top valence states, i.e. holes, do not play Rashba splitting, unless the original VBM band is surpassed by the upward surface bands as shown in figure 4(c).

The Rashba parameter of this 2D bilayer halide perovskite seems unusual, since for those 3D organic–inorganic hybrid metal halide perovskites it has been demonstrated for both electrons and holes do not show too much difference in their Rashba parameters [44]. For other materials of BiTeI [18],

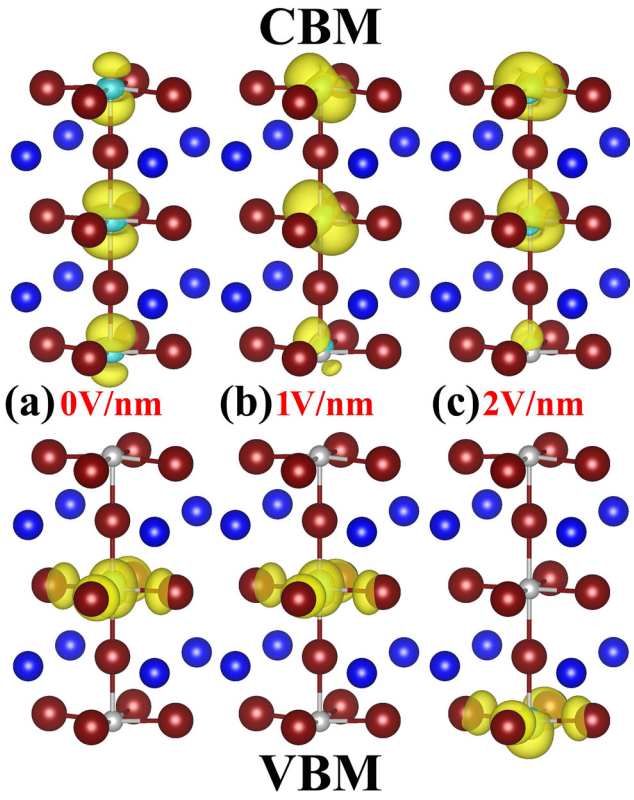

Figure 4. The partial charge densities of CBM and VBM the $PbBr_2$-terminated bilayer under EEF of 0, 1, and 2 V nm^{-1}. (Cyan: negative isosurface for electron deficit region; yellow: positive isosurface for electron increased region).

GeTe [19], black phosphorus [45], and organic–inorganic halide perovskites [25, 28], their Rashba splitting always happens for both CBM and VBM bands. This asymmetric Rashba effect can be ascribed to the reversion transition of the upper valence bands of this 2D $CsPbBr_3$ bilayer. Figure 5(a) presents the electronic bands for the $PbBr_2$ terminated bilayer in its bulk atom positions, together with charge densities of its top three double-degenerate valence bands at point-M. Without surface relaxation, the VBM state actually comes from the surface states rather than the central layer one as presented in figure 3(a). As expected, it is SOC that removes the double degeneracy of the top valence bands of the relaxed bilayer, as shown in figure 5(b).

3.3. Bandgaps and Rashba parameters of CBM

As a result of the reversion of top VBM bands, the nature of this bilayer bandgap changes consequently. As shown in figure 3(a), the $PbBr_2$ terminated bilayer has the intrinsic direct bandgap initially. As EEF turned on, the bandgap becomes indirect, and goes to direct again after EEF gets over the band-interchange point, as shown in figures 3(b)–(f). In figure 6, we plotted the EEF-dependent bandgap, together with the calculated Rashba parameter from the CBM band. Basically, the bandgap decreases monotonically with the increasing EEF, but the gap value drops dramatically after the

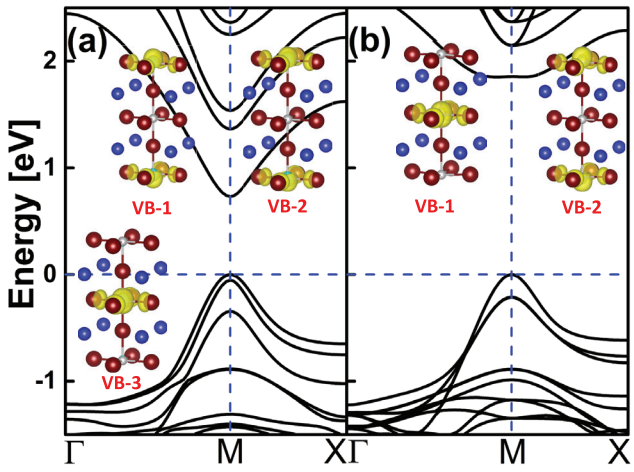

Figure 5. The calculated electronic band structures of the $PbBr_2$-terminated bilayer without EEF, together with the partial charge densities of top valence bands (top 1:VB-1, top 2:VB-2, top 3: VB-3) at point M, in cases of (a): without surface relaxation and with SOC; and (b): with surface relaxation and without SOC.

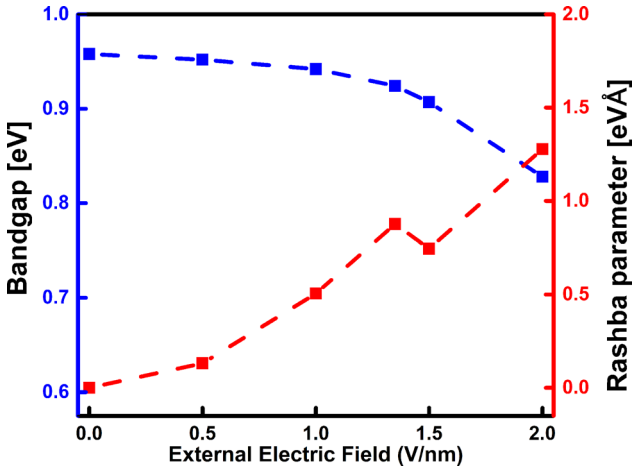

Figure 6. The calculated bandgaps and Rashba parameters of CBM with a series of EEF (blue: bandgap; red: Rashba parameter).

VBM transition point. Overall, that can be understood as the Stark effect [46–48].

Interestingly, the VBM-band switch also affects the dependence of the CBM Rashba parameter on EEF. Before this VBM flip, the CBM Rashba parameter increases continuously with EEF and reaches the maximum of 0.88 eV Å at EEF of 1.35 V nm^{-1}. After that, the Rashba parameter curve shows a kink, and then it increases with EEF again. The reason for this kink is that the VBM state located at the central layer is transformed into the surface layer when EEF is larger than 1.35 V nm^{-1}, such as VBM state at the 2 V nm^{-1} which is shown in figure 4(c). Experimentally, the Rashba parameters of $CsPbBr_3$ were measured on nanocrystals by analysing their excitonic magneto-photoluminescence spectra [33]. With the applied magnetic field from 0 to 8 Tesla, they found 0.2 and 0.05 eV Å for the Rashba coefficient for electrons and holes respectively. Obviously, the Rashba effect is more tunable for $CsPbBr_3$ in the layer structure with the electric field. But this

seems only true for those $CsPbBr_3$ layers with the proper surfaces. We found that the Rashba splitting is negligible with EEF for the $CsPbBr_3$ bilayer that is terminated with CsBr surface, as shown in figure 2(b) and the supplementary material (stacks.iop.org/JPhysCM/30/265501/mmedia).

4. Conclusions

In summary, by theoretically examining the spin-polarized electronic bands of 2D $CsPbBr_3$ bilayers with the vertically applied electric field, we have identified the asymmetric Rashba splitting upon charge carrier type on the $PbBr_2$ terminated bilayer. It is surface relaxation that lowers the energy of the original two top valence bands and makes the original top three valence one the VBM band. While the updated VBM electronic state is protected by the surface charges and with high symmetry, the holes of this 2D $CsPbBr_3$ bilayers are inert to EEF until the surface valence bands reverse back to the top at the EEF of 1.35 V nm^{-1}. The reversion of top VBM bands also makes the 2D $CsPbBr_3$ bilayer possess the indirect bandgap nature once EEF turned on and regain the direct style after the VBM transtion. In making spintronic devices, only n-type carriers in this 2D material will yield to the EEF-induced Rashba splitting, with the maximum parameter of 0.88 eV Å at EEF of 1.35 V nm^{-1}. For the 2D layers with very large surface to bulk ratio, normally the surface relaxation will remarkably reduce the energy of the system, that act mainly on the top valence bands for stoichiometric materials. That may hint that the n-type Rashba effect could be universally observed on the similar 2D perovskites with proper surfaces selected. That may give these 2D materials unique advantages in making advanced functional spin devices, such as in blocking undesired p-type spins.

Acknowledgment

LL acknowledges the support from the National Science Fund for Distinguished Young Scholars of China (No. 61525404).

ORCID iDs

Xuejiao Chen https://orcid.org/0000-0002-9230-3046

References

[1] Szuromi P and Grocholski B 2017 *Science* **358** 732–3
[2] Zhao Y C, Zhou W K, Zhou X, Liu K H, Yu D P and Zhao Q 2016 *Light Sci. Appl.* **6** e16243
[3] Xie C, You P, Liu Z, Li L and Yan F 2017 *Light Sci. Appl.* **6** e17023
[4] De Wolf S, Holovsky J, Moon S J, Loper P, Niesen B, Ledinsky M, Haug F J, Yum J H and Ballif C 2014 *J. Phys. Chem. Lett.* **5** 1035–9
[5] Wehrenfennig C, Eperon G E, Johnston M B, Snaith H J and Herz L M 2014 *Adv. Mater.* **26** 1584–9
[6] Dong Q F, Fang Y J, Shao Y C, Mulligan P, Qiu J, Cao L and Huang J S 2015 *Science* **347** 967–70
[7] Miyata A, Mitioglu A, Plochocka P, Portugall O, Wang J T W, Stranks S D, Snaith H J and Nicholas R J 2015 *Nat. Phys.* **11** 582–7
[8] Yin W J, Shi T and Yan Y 2014 *Appl. Phys. Lett.* **104** 063903
[9] Kovalenko M V, Protesescu L and Bodnarchuk M I 2017 *Science* **358** 745C750
[10] Dresselhaus G 1955 *Phys. Rev.* **100** 580–6
[11] Bychkov Y A and Rashba E I 1984 *JETP Lett.* **39** 78–81
[12] Rashba E I 1960 *Sov. Phys.—Solid State* **2** 1109–22
[13] Grundler D 2000 *Phys. Rev. Lett.* **84** 6074–7
[14] Ganichev S D *et al* 2004 *Phys. Rev. Lett.* **92** 256601
[15] Averkiev N S, Golub L E, Gurevich A S, Evtikhiev V P, Kochereshko V P, Platonov A V, Shkolnik A S and Efimov Y P 2006 *Phys. Rev.* B **74** 033305
[16] Meier L, Salis G, Shorubalko I, Gini E, Schön S and Ensslin K 2007 *Nat. Phys.* **3** 650–4
[17] Dil J H, Meier F, Lobo-Checa J, Patthey L, Bihlmayer G and Osterwalder J 2008 *Phys. Rev. Lett.* **101** 266802
[18] Ishizaka K *et al* 2011 *Nat. Mater.* **10** 521–6
[19] Di Sante D, Barone P, Bertacco R and Picozzi S 2013 *Adv. Mater.* **25** 509–13
[20] Shanavas K V and Satpathy S 2014 *Phys. Rev. Lett.* **112** 086802
[21] Zhang X, Liu Q, Luo J W, Freeman A J and Zunger A 2014 *Nat. Phys.* **10** 387–93
[22] Santander-Syro A F, Fortuna F, Bareille C, Rodel T C, Landolt G, Plumb N C, Dil J H and Radovic M 2014 *Nat. Mater.* **13** 1085–90
[23] Motta C, El-Mellouhi F, Kais S, Tabet N, Alharbi F and Sanvito S 2015 *Nat. Commun.* **6** 7026
[24] Kepenekian M, Robles R, Katan C, Sapori D, Pedesseau L and Even J 2015 *ACS Nano.* **9** 11557–67
[25] Zheng F, Tan L Z, Liu S and Rappe A M 2015 *Nano Lett.* **15** 7794–800
[26] Leppert L, Reyes-Lillo S E and Neaton J B 2016 *J. Phys. Chem. Lett.* **7** 3683–9
[27] Hutter E M, Gelvez-Rueda M C, Osherov A, Bulovic V, Grozema F C, Stranks S D and Savenije T J 2016 *Nat. Mater.* **16** 115
[28] Etienne T, Mosconi E and De Angelis F 2016 *J. Phys. Chem. Lett.* **7** 1638–45
[29] Niesner D, Wilhelm M, Levchuk I, Osvet A, Shrestha S, Batentschuk M, Brabec C and Fauster T 2016 *Phys. Rev. Lett.* **117** 126401
[30] Moser J E 2016 *Nat. Mater.* **16** 4–6
[31] Zhai Y X, Baniya S, Zhang C, Li J W, Haney P, Sheng C X, Ehrenfreund E and Vardeny Z V 2017 *Sci. Adv.* **3** e1700704
[32] Wang Z, Shi Z, Li T, Chen Y and Huang W 2016 *Angew. Chem. Int. Ed. Engl.* **56** 1190–212
[33] Isarov M, Tan L Z, Bodnarchuk M I, Kovalenko M V, Rappe A M and Lifshitz E 2017 *Nano Lett.* **17** 5020–6
[34] Becker M A *et al* 2018 *Nature* **553** 189–93
[35] Akkerman Q A *et al* 2016 *J. Am. Chem. Soc.* **138** 1010–6
[36] Bekenstein Y, Koscher B A, Eaton S W, Yang P and Alivisatos A P 2015 *J. Am. Chem. Soc.* **137** 16008
[37] Kresse G and Joubert D 1999 *Phys. Rev.* B **59** 1758–75
[38] Blochl P E 1994 *Phys. Rev.* B **50** 17953–79
[39] Perdew J P, Burke K and Ernzerhof M 1996 *Phys. Rev. Lett.* **77** 3865–8
[40] Kresse G and Furthmuller J 1996 *Phys. Rev.* B **54** 11169–86
[41] Kresse G and Hafner J 1993 *Phys. Rev.* B **47** 558–61
[42] Moller C K 1958 *Nature* **182** 1436
[43] Koelling D D and Harmon B N 1977 *J. Phys. C: Solid State Phys.* **10** 3107
[44] Kim M, Im J, Freeman A J, Ihm J and Jin H 2014 *Proc. Natl Acad. Sci. USA* **111** 6900–4
[45] Popović Z S, Kurdestany J M and Satpathy S 2015 *Phys. Rev.* B **92** 035135
[46] O'Keeffe J, Wei C and Cho K 2002 *Appl. Phys. Lett.* **80** 676–8
[47] Zhang Z and Guo W 2008 *Phys. Rev.* B **77** 075403
[48] Liu Q, Li L, Li Y, Gao Z, Chen Z and Lu J 2012 *J. Phys. Chem.* C **116** 21556–62